

Constraints on quasar broad line regions from microlensing

*Damien Hutsemékers¹,
L. Braibant¹, D. Sluse¹, T. Anguita², R. Goosmann³*

¹Université de Liège, Belgium

²Universidad Andrés Bello, Chile

³Observatoire de Strasbourg, France

Outline

- Gravitational microlensing and the quasar inner structure
- Observation of line profile deformations. Constraints on the broad emission line region (BELR)
- BELR models and microlensing simulations. Confrontation with observations
- Microlensing constraints on the BAL and scattering regions

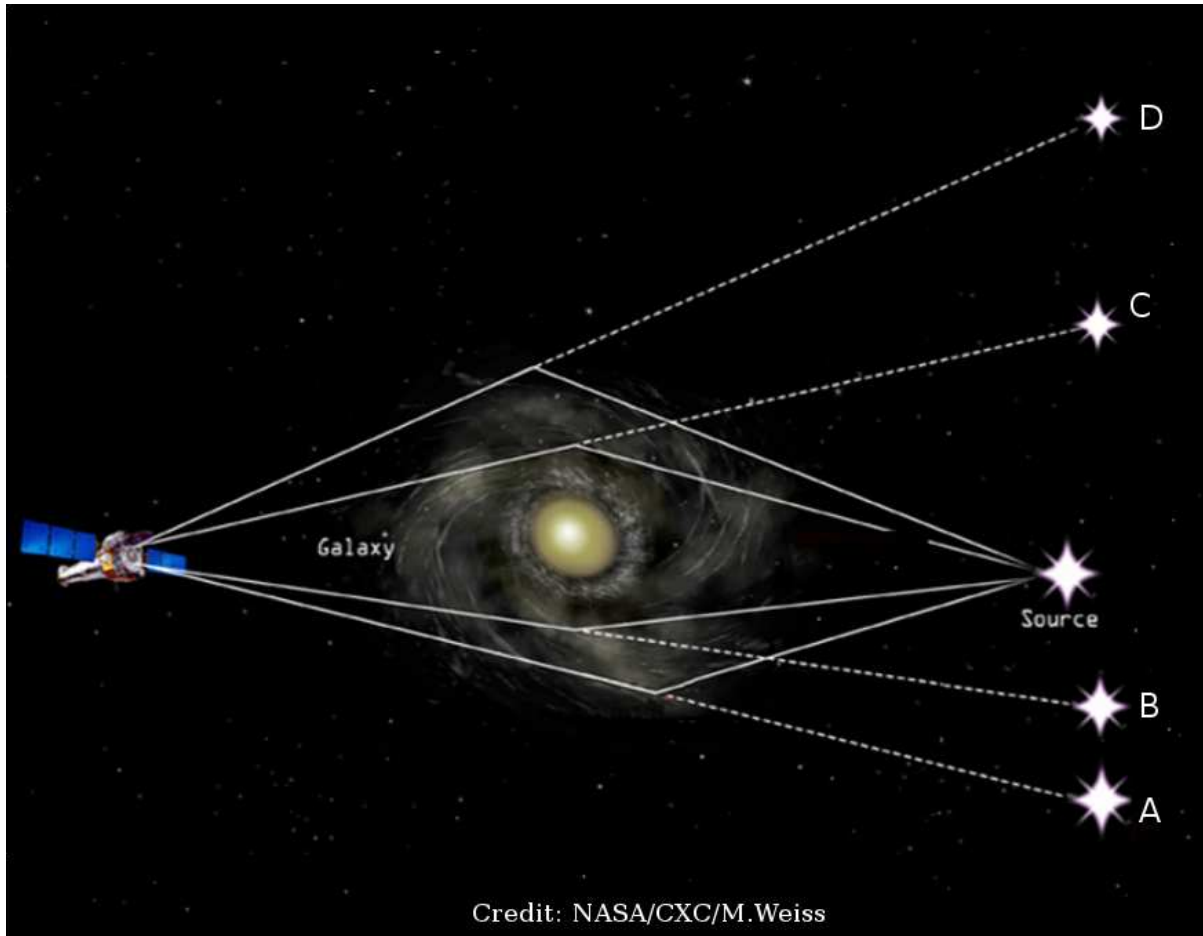
Based on:

- Braibant, Hutsemékers, Sluse, Anguita et al. 2014, A&A 565, L11
- Sluse, Hutsemékers, Braibant, Anguita et al. 2015, A&A 582, A109
- Hutsemékers, Sluse, Braibant, Anguita 2015, A&A 584, A61
- Braibant, Hutsemékers, Sluse, Anguita 2016, A&A 592, A23
- Braibant, Hutsemékers, Sluse, Goosmann 2017, in preparation

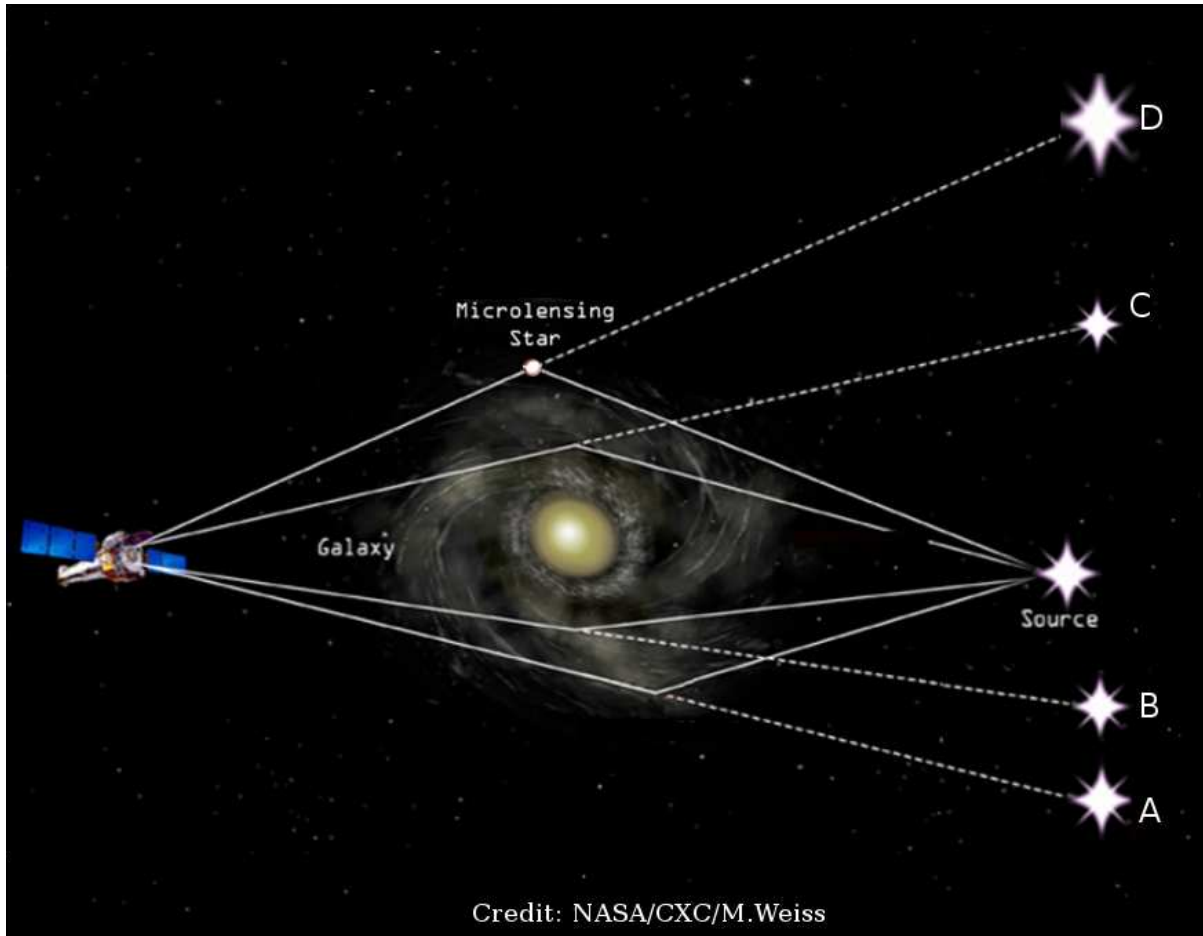
See also:

- Abajas, Mediavilla, Munoz, Popovic et al. 2002, ApJ 576, 640
- O'Dowd, Bate, Webster, Labrie et al. 2015, ApJ 813, 62
- Motta, Mediavilla, Rojas, Falco et al. 2017, ApJ 835, 132

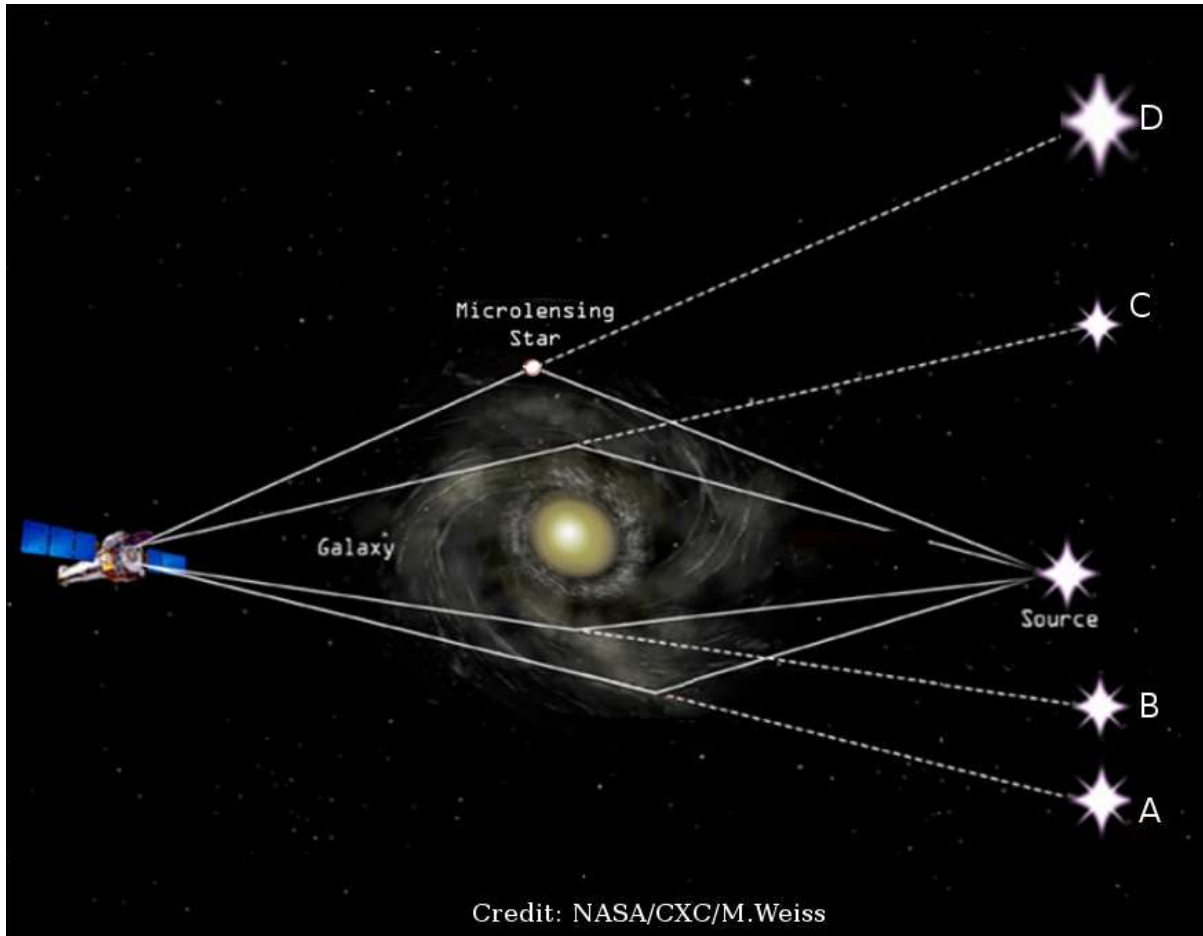
Gravitational microlensing



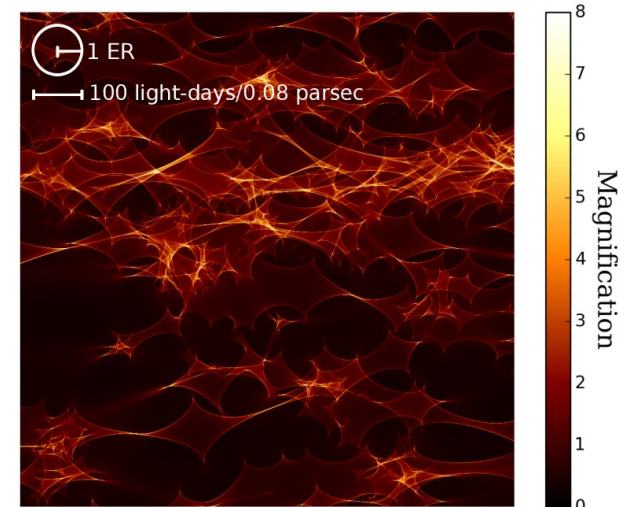
Gravitational microlensing



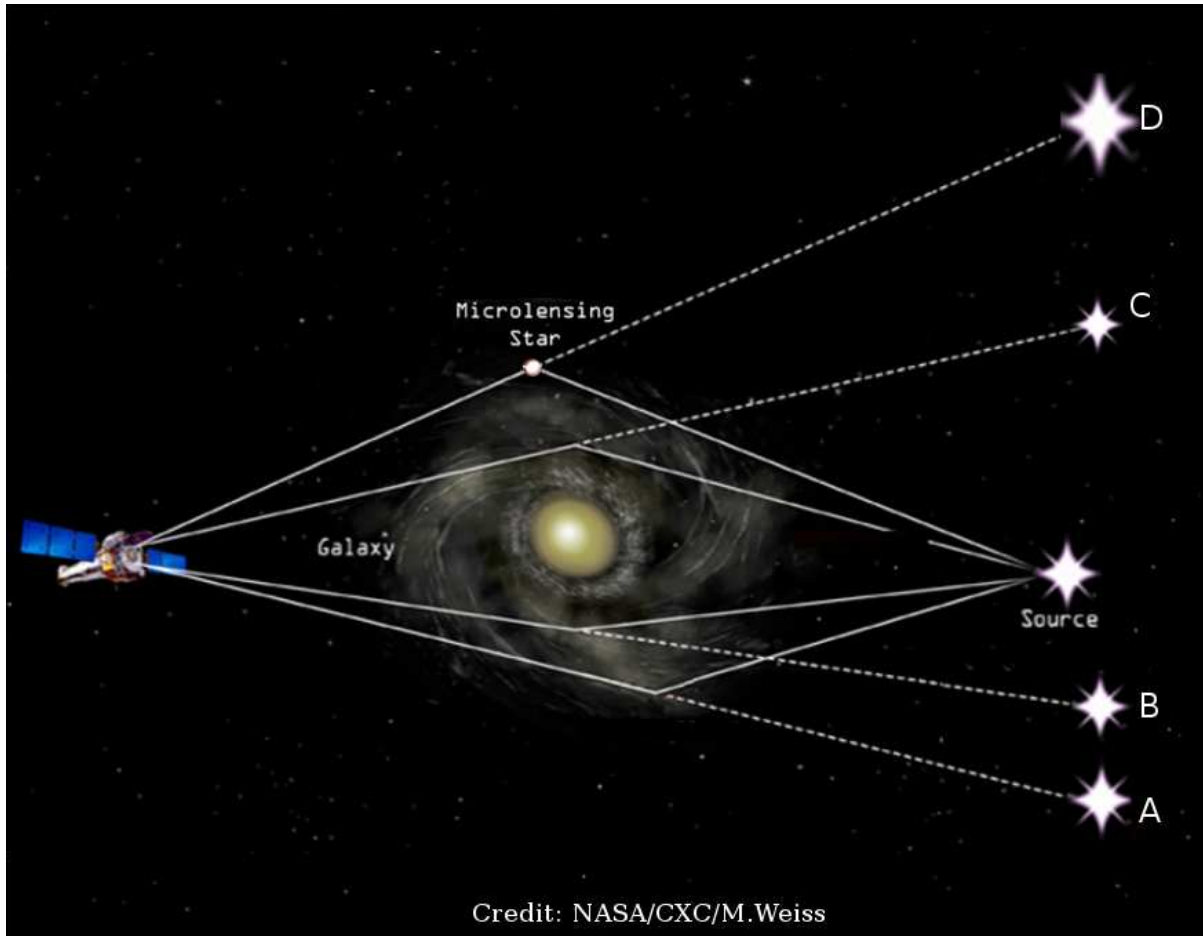
Gravitational microlensing



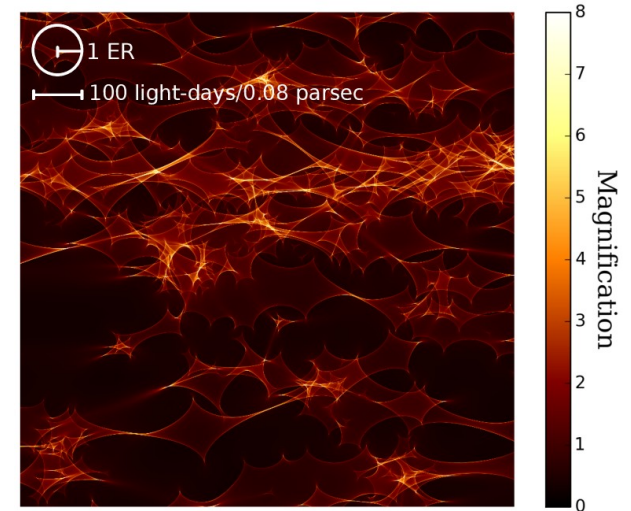
Galaxy tidal field + multiple stars
> complex magnification pattern



Gravitational microlensing



Galaxy tidal field + multiple stars
> complex magnification pattern



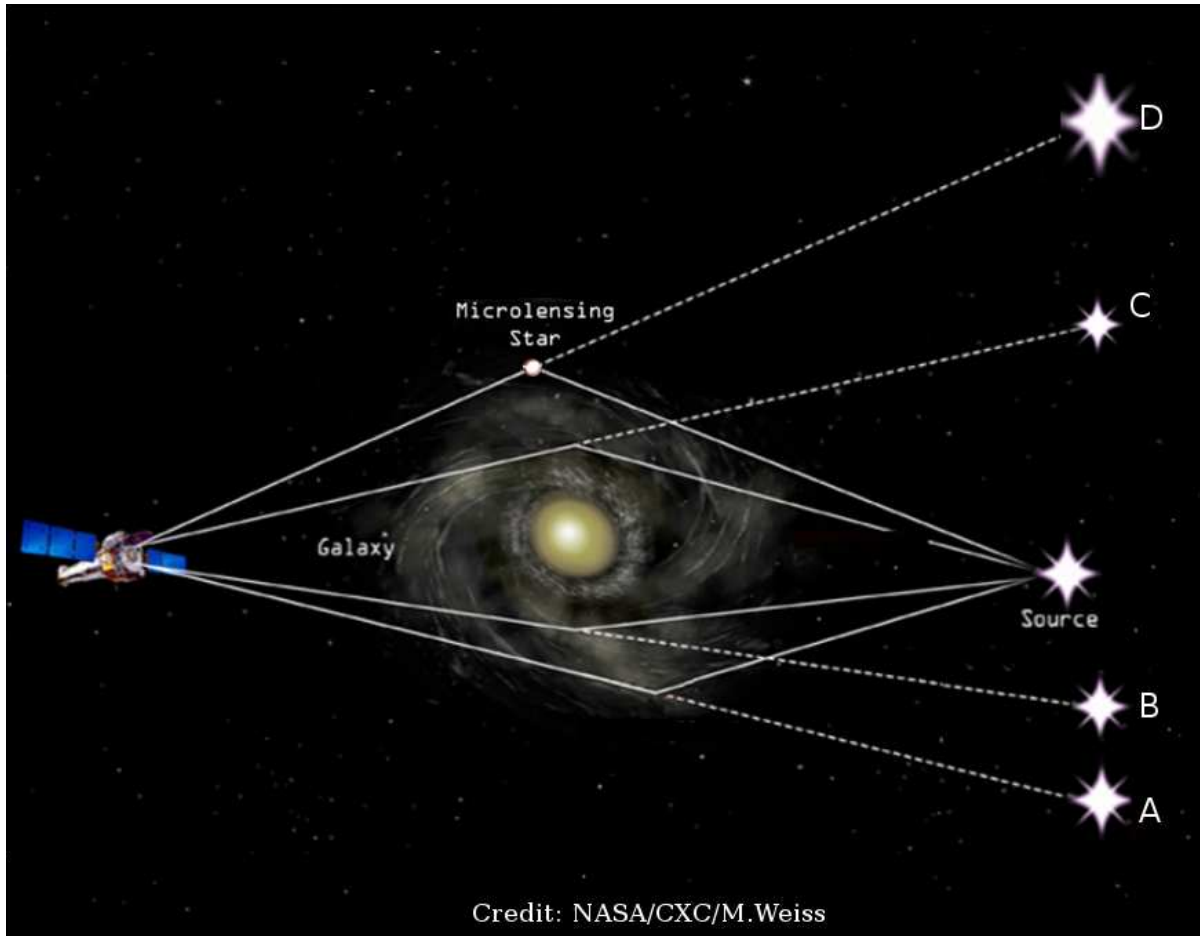
$$\mu \sim 1 + \sqrt{r_E/r_s}$$

$$r_E \sim \sqrt{M} \sqrt{D_s D_{ls}/D_l}$$

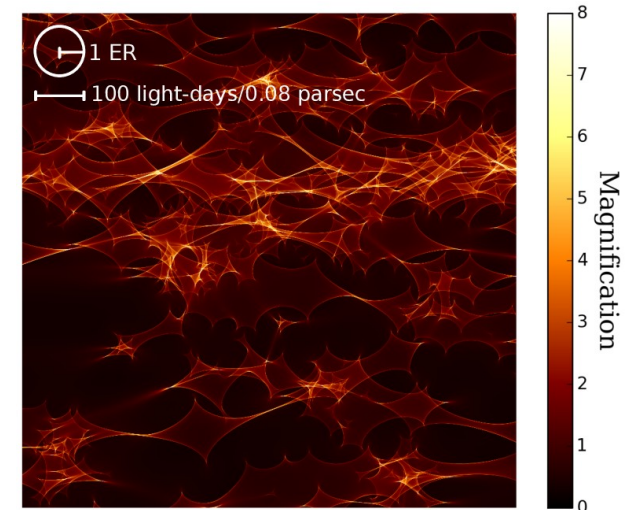
$$r_E \sim 15 \sqrt{M/M_{Sun}} \text{ ld}$$

for $z_l=0.5$ $z_s=2.0$

Gravitational microlensing



Galaxy tidal field + multiple stars
> complex magnification pattern

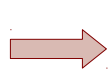


$$\mu \sim 1 + \sqrt{r_E/r_s}$$

$$r_E \sim \sqrt{M} \sqrt{D_s D_{ls}/D_l}$$

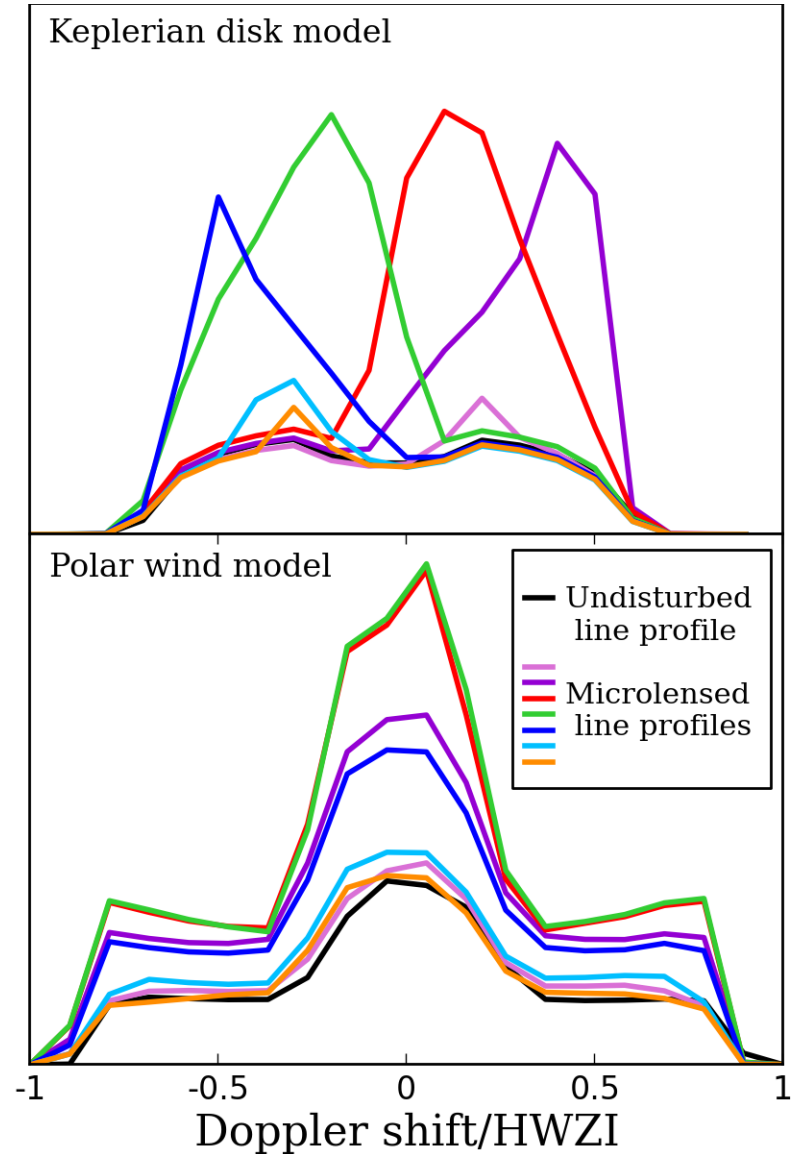
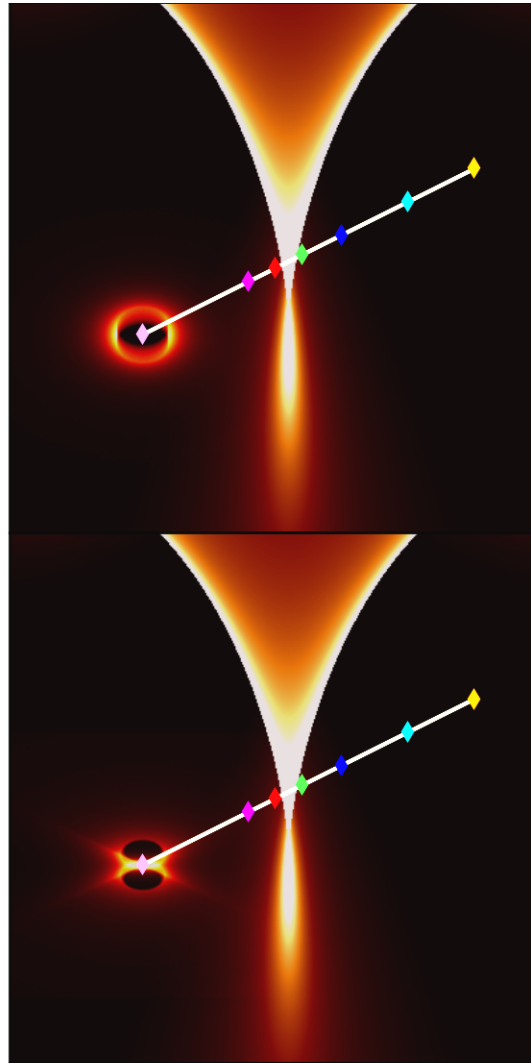
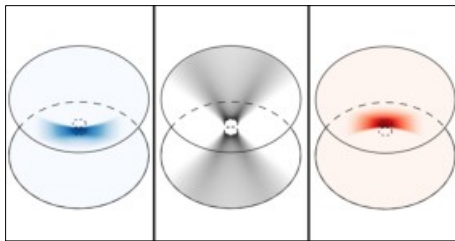
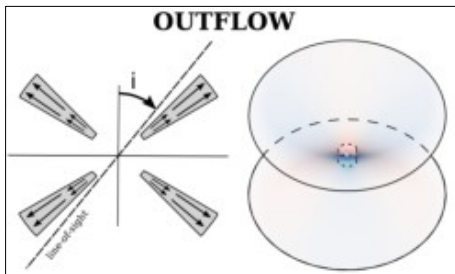
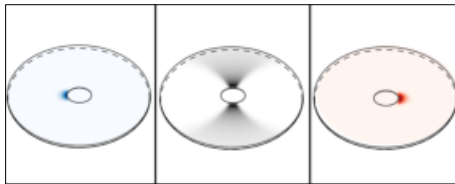
$$r_E \sim 15 \sqrt{M/M_{Sun}} \text{ ld}$$

for $z_l=0.5$ $z_s=2.0$

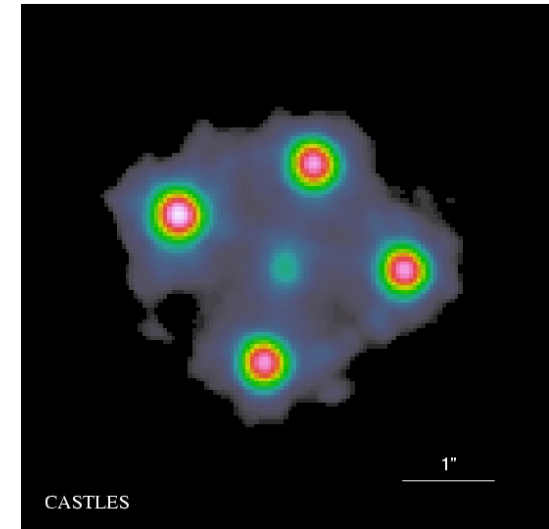
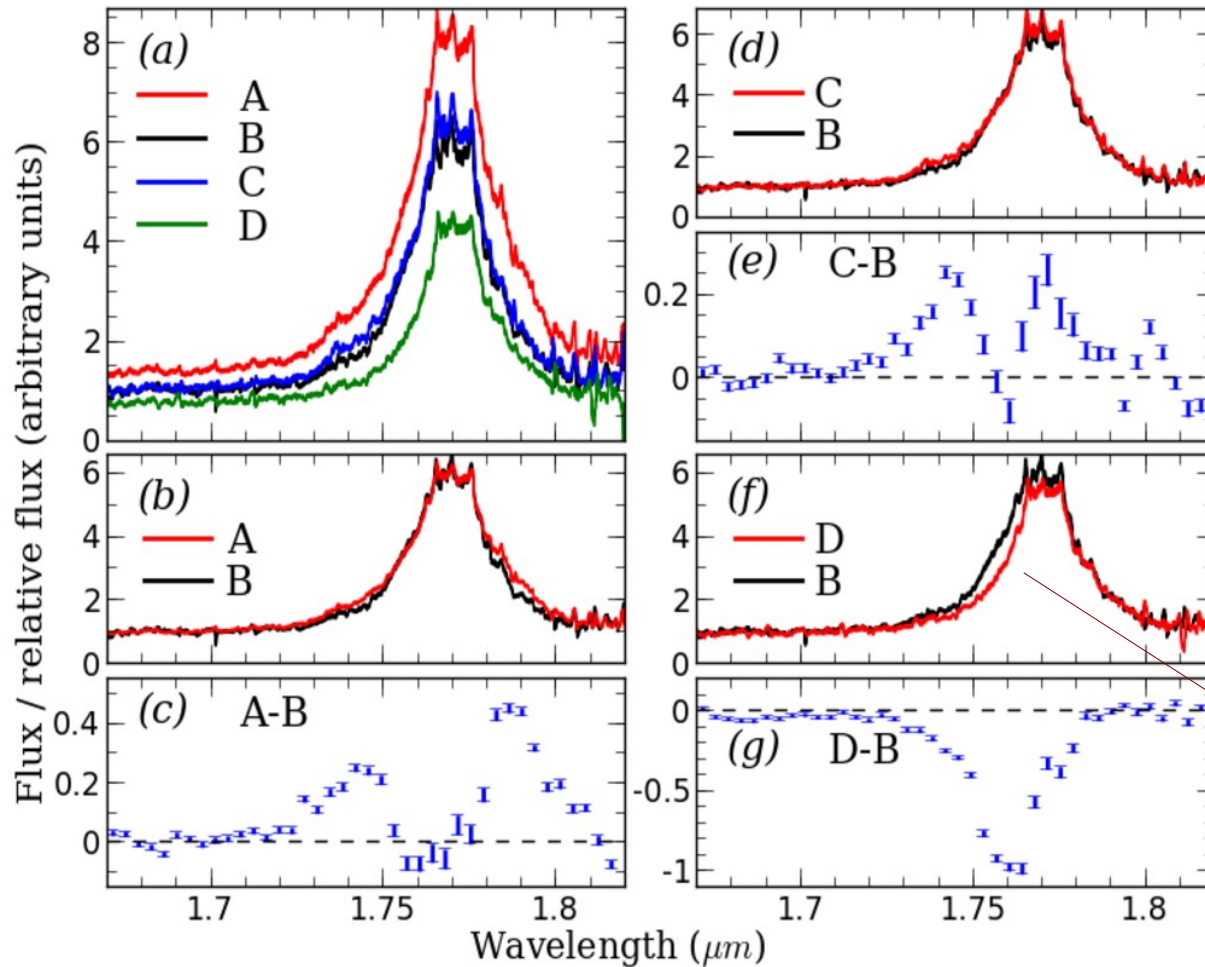


Important constraints on the accretion disk size and temperature structure
(e.g., Blackburne et al. 2011, Jiménez-Vicente et al. 2014)

Microlensing of the BELR



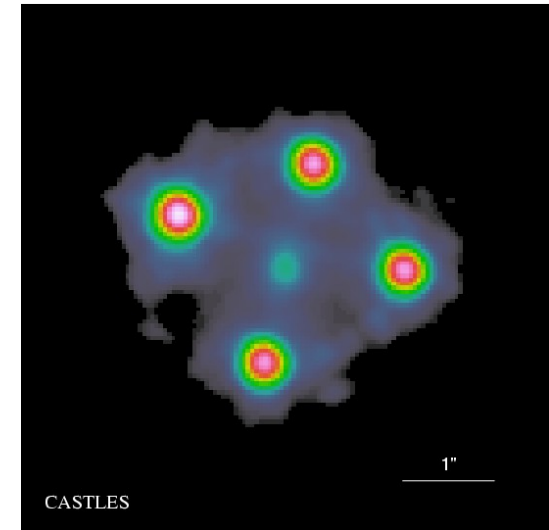
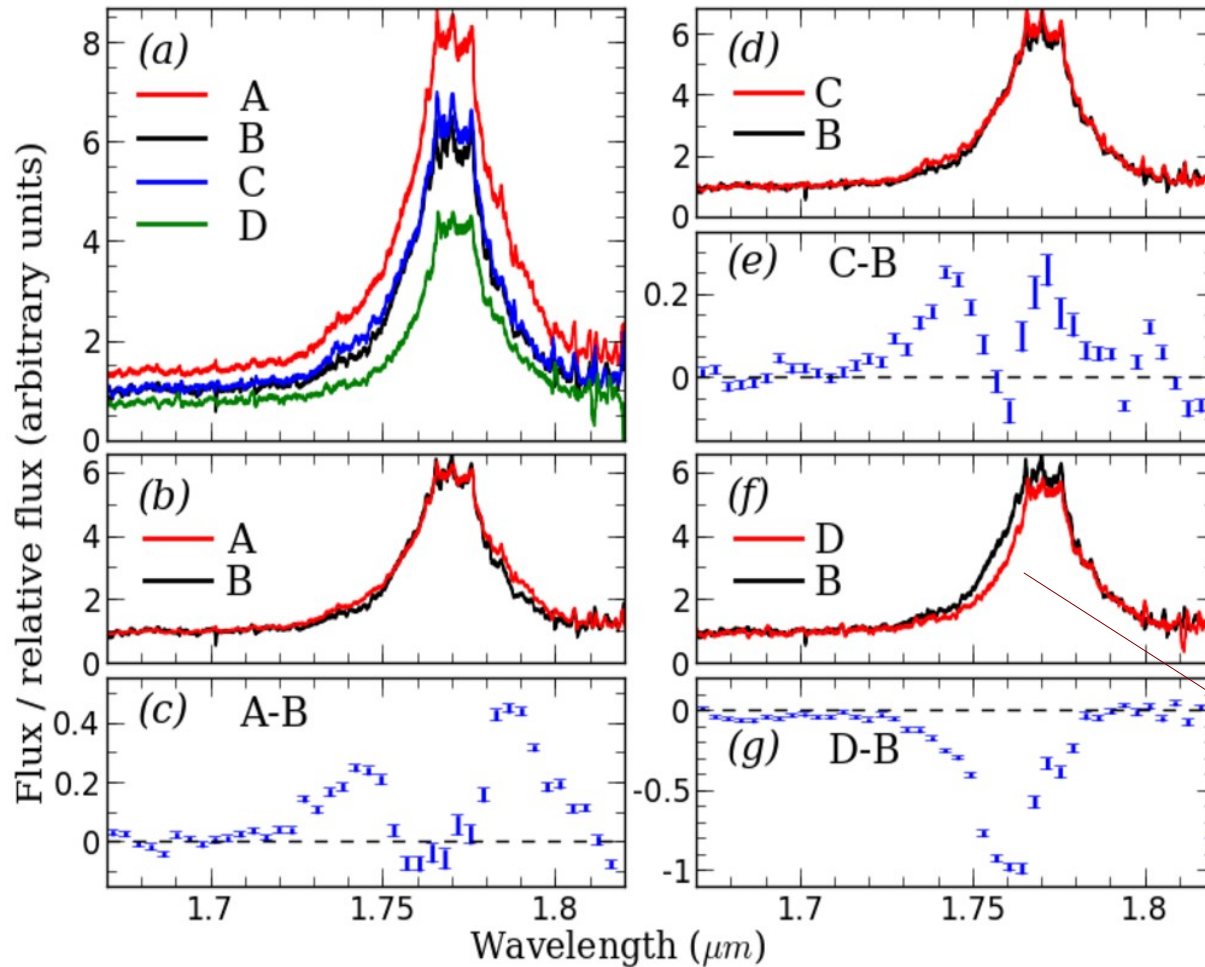
Microlensing of H α in HE0435-1223



$$z_s = 1.7 \quad z_l = 0.5$$

Strong microlensing effect in the spectrum of image D (image B is not microlensed)

Microlensing of H α in HE0435-1223



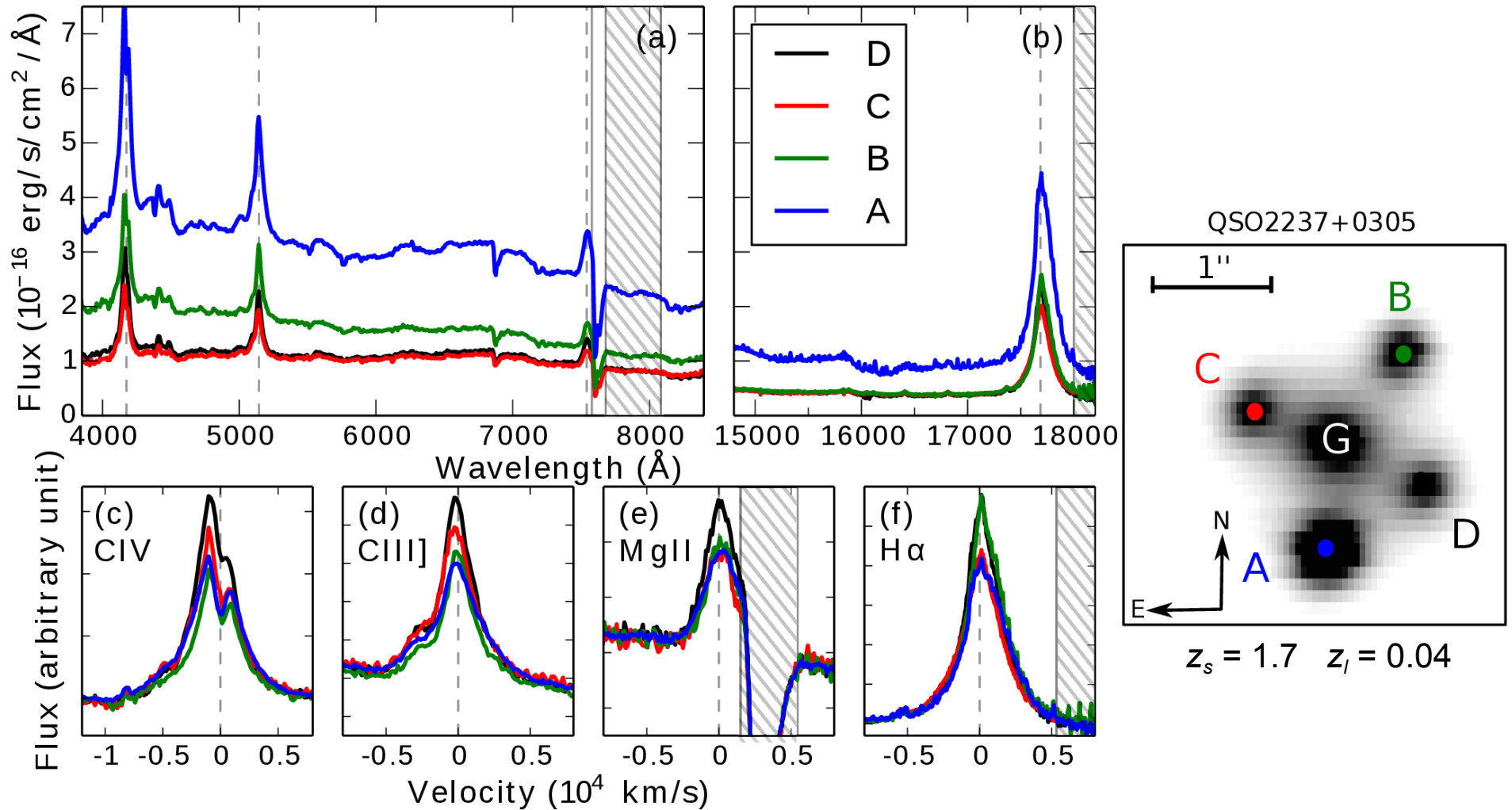
$$z_s = 1.7 \quad z_l = 0.5$$

Strong microlensing effect in the spectrum of image D (image B is not microlensed)

Microlensing of the BELR is common in lensed quasars

(Sluse et al. 2012, Guerras et al 2013)

Microlensing in the Einstein Cross

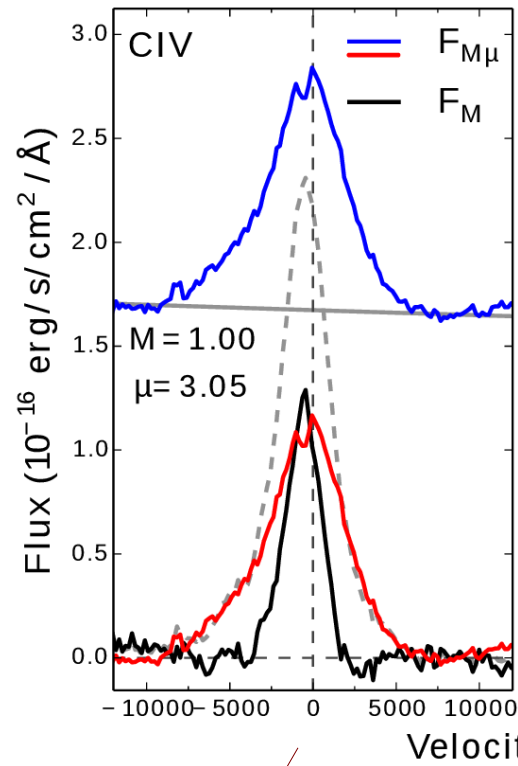


Visible and near-infrared observations obtained *at the same epoch*

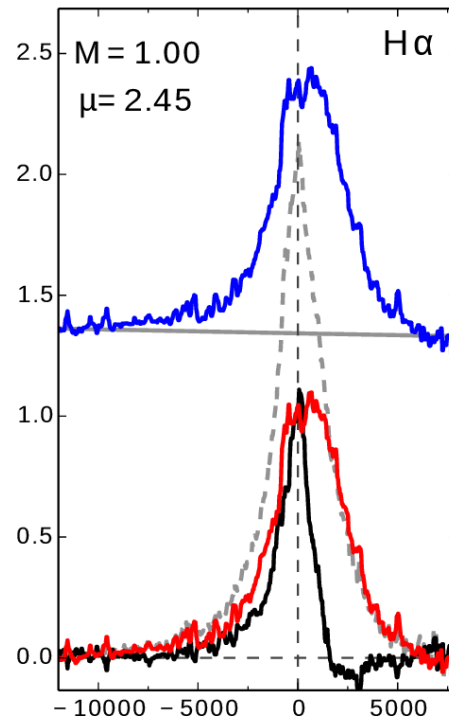
Microlensing in the Einstein Cross

The part of the line profile affected by microlensing can be disentangled from the part not affected, using the spectra of two images, one microlensed and the other one not

high
ionization



Wings microlensed,
Core not

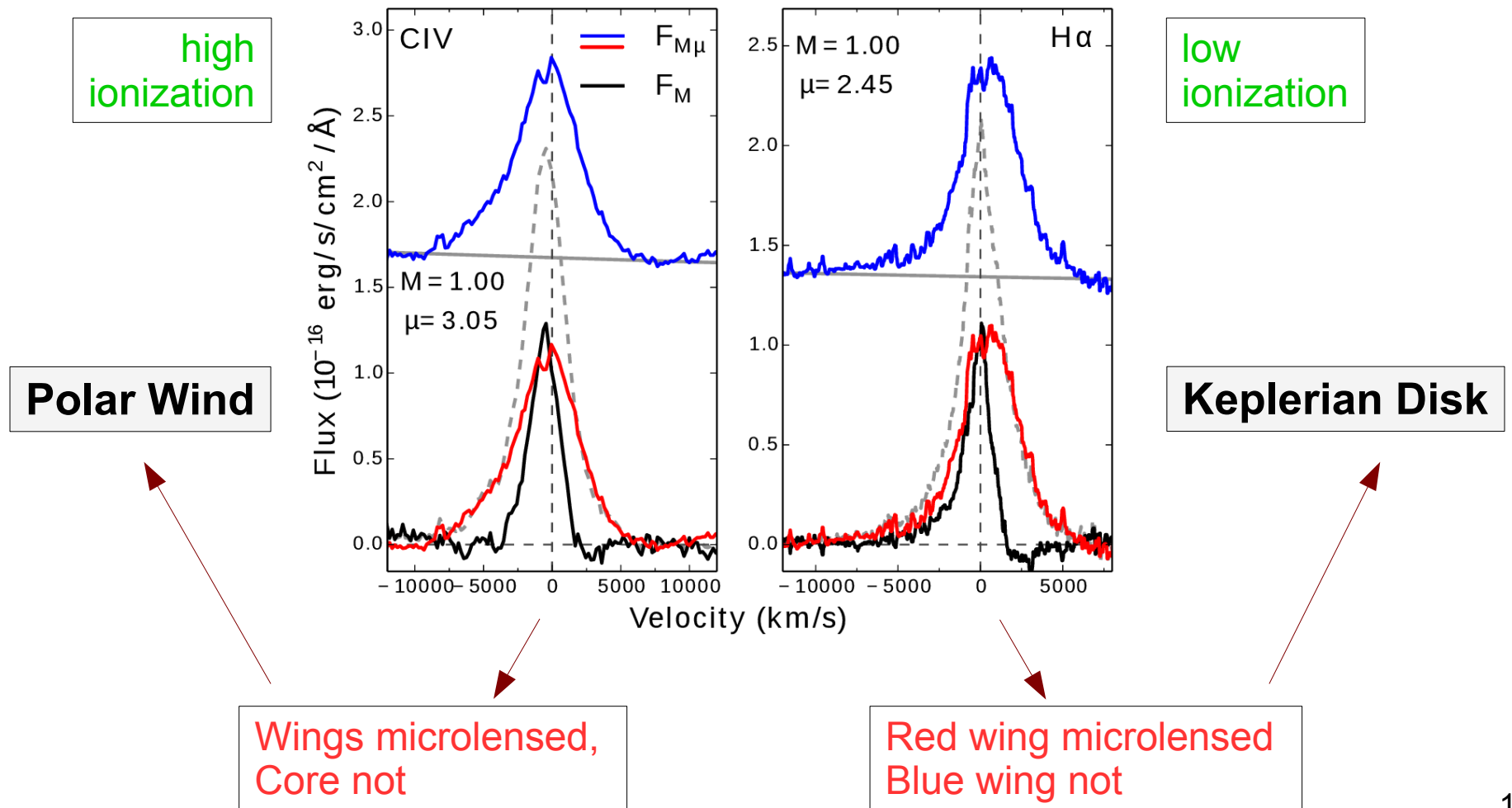


low
ionization

Red wing microlensed
Blue wing not

Microlensing in the Einstein Cross

The part of the line profile affected by microlensing can be disentangled from the part not affected, using the spectra of two images, one microlensed and the other one not



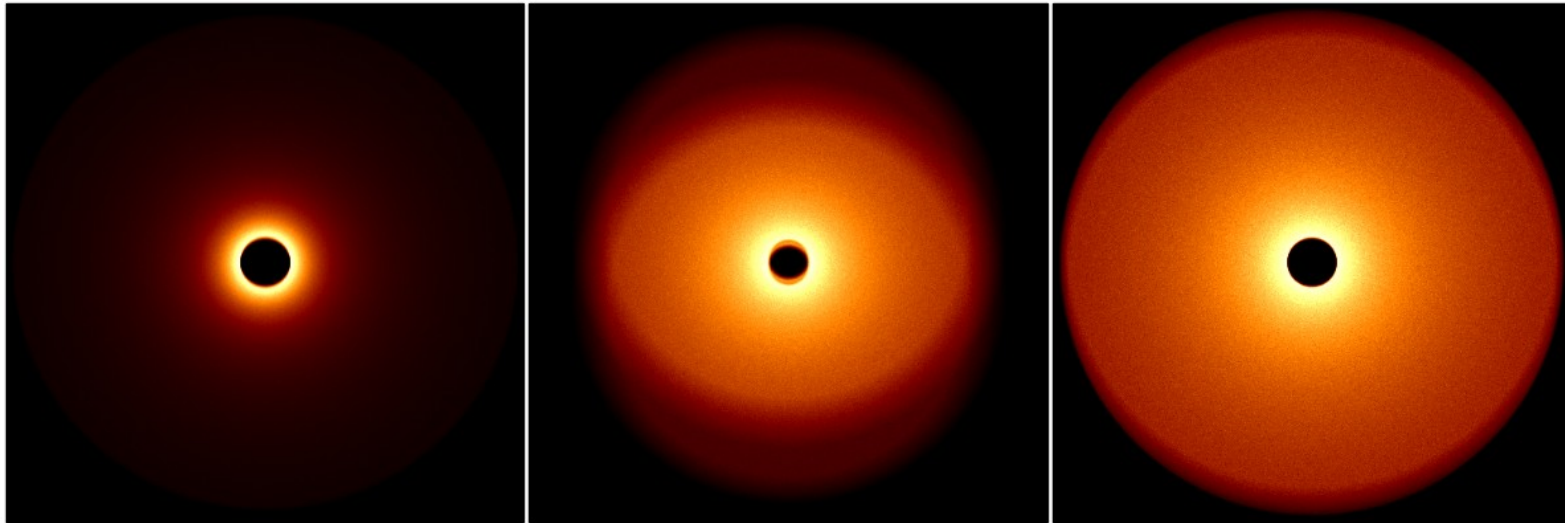
BELR models and microlensing simulations

→ The BELR is modeled with the Monte-Carlo radiative transfer code STOKES (Goosmann et al.)

→ Keplerian disk

Polar wind

Equatorial wind



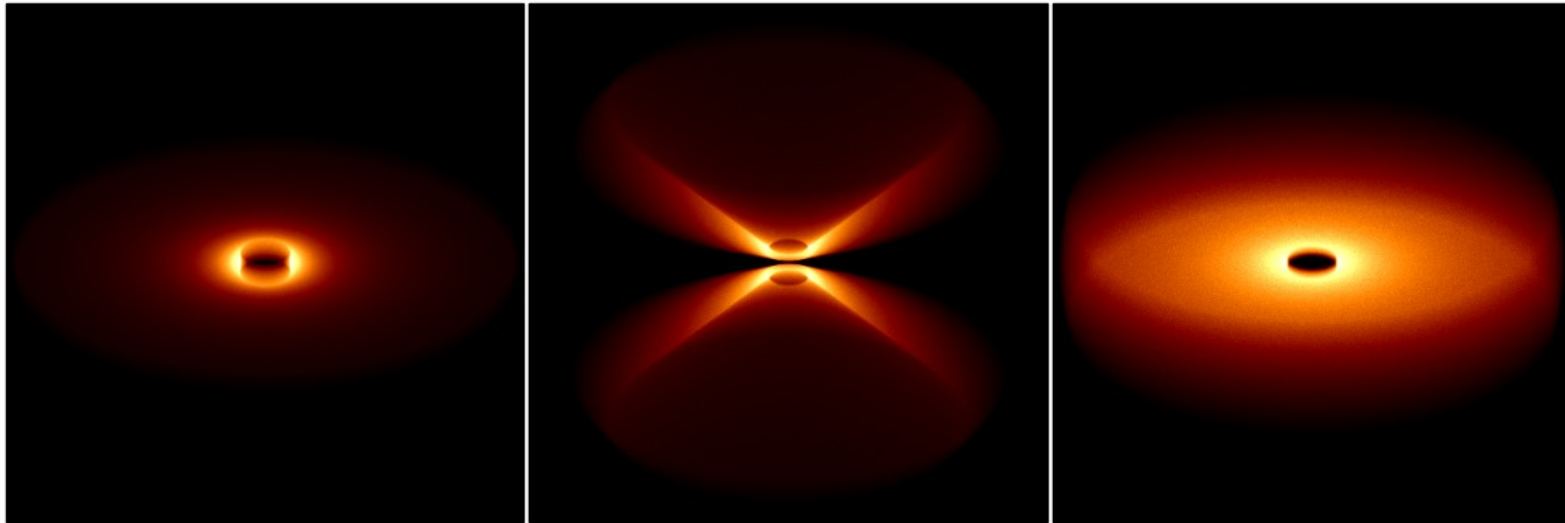
BELR models and microlensing simulations

→ The BELR is modeled with the Monte-Carlo radiative transfer code STOKES (Goosmann et al.)

→ Keplerian disk

Polar wind

Equatorial wind



with various inclinations, sizes, emissivities

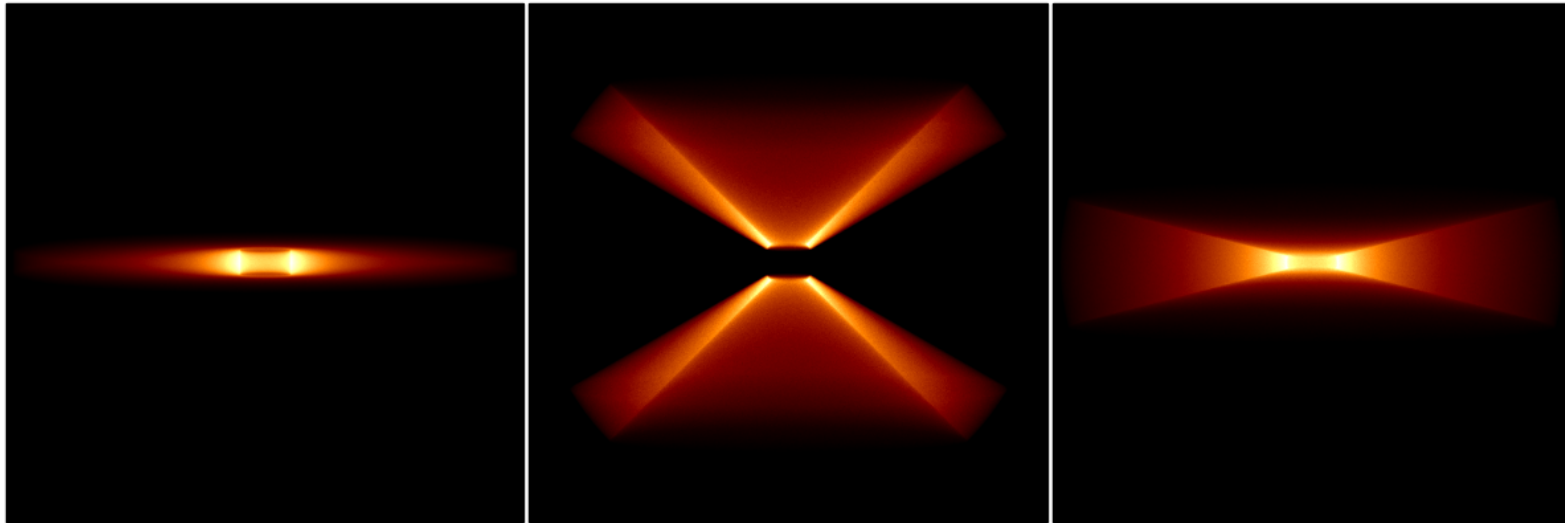
BELR models and microlensing simulations

→ The BELR is modeled with the Monte-Carlo radiative transfer code STOKES (Goosmann et al.)

→ Keplerian disk

Polar wind

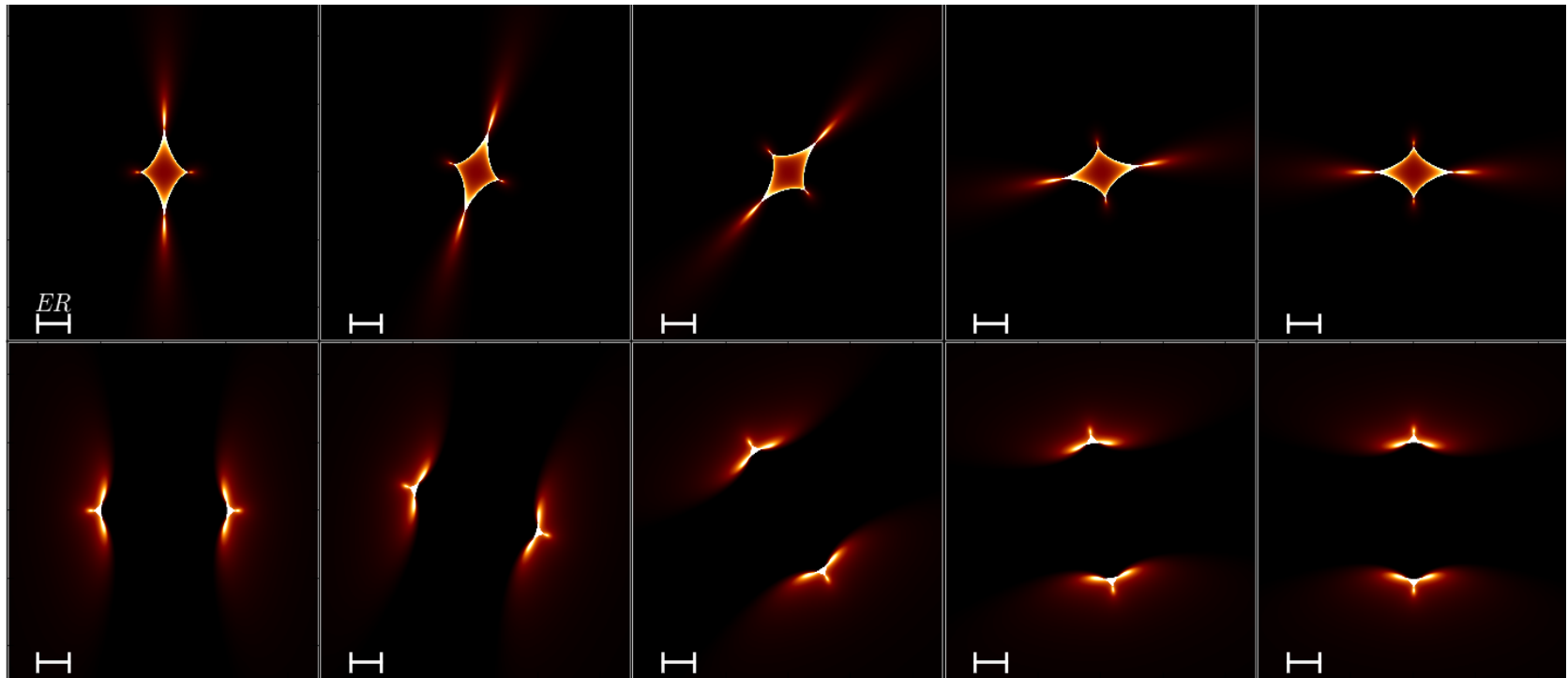
Equatorial wind



with various inclinations, sizes, emissivities

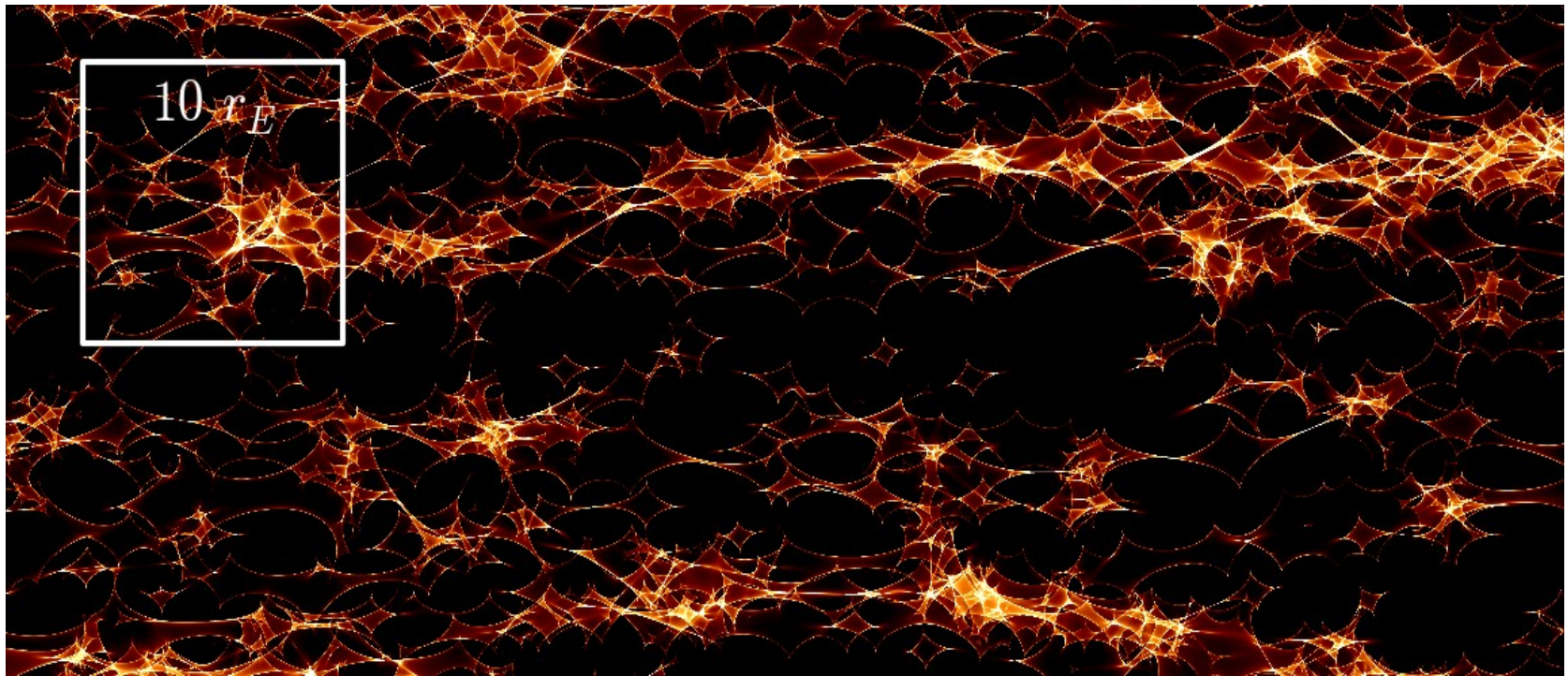
BELR models and microlensing simulations

- Computed monochromatic images of the BELR are convolved with microlensing amplification maps
- Magnification maps : generic Chang-Refsdal caustics



BELR models and microlensing simulations

- Computed monochromatic images of the BELR are convolved with microlensing amplification maps
- or complex patterns



BELR models and microlensing simulations

→ Microlensed emission line profiles are reconstructed at each position on the magnification maps

→ The continuum source is simultaneously modeled and magnified by the same caustics

→ The thousands of simulated profiles are characterized by four observable quantities :

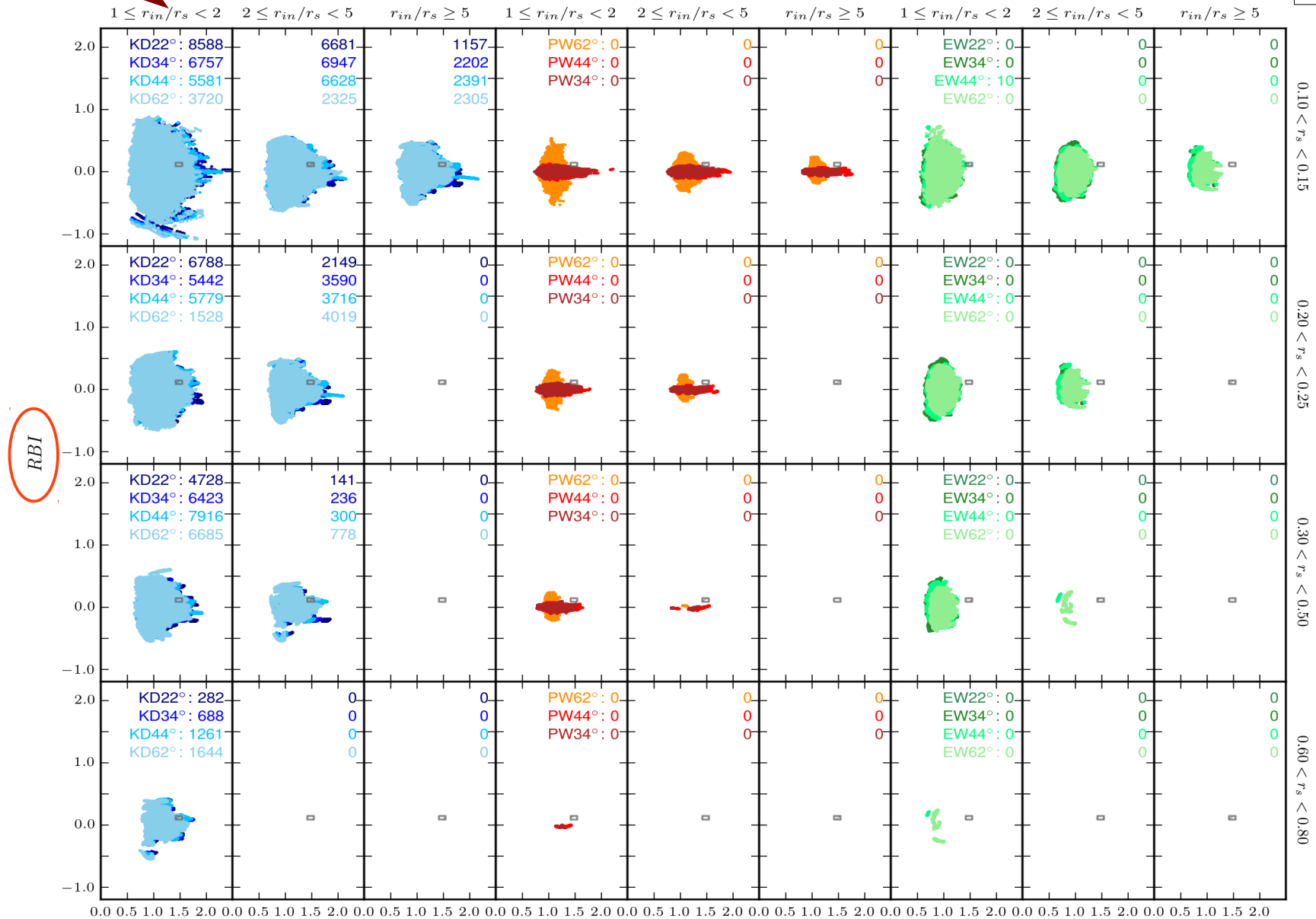
- μ_{cont} , the magnification of the continuum source
- μ_{blr} , the total magnification of the emission line
- **WCI**, the wing/core index measuring the amplification of the wings with respect to the core of the line
- **RBI**, the red/blue index measuring the amplification of the line red wing with respect to the blue wing

Confrontation to observations

BELR radius

Modeling the distortions of the H α line profile in Q2237+0305A
 Microlensing by a ($\kappa = 0.394, \gamma = 0.395$) caustic network $\rightarrow 2.20 < \mu^{cont} < 2.70, 2.09 < \mu^{BLR} < 2.35$

Continuum source radius



RBI

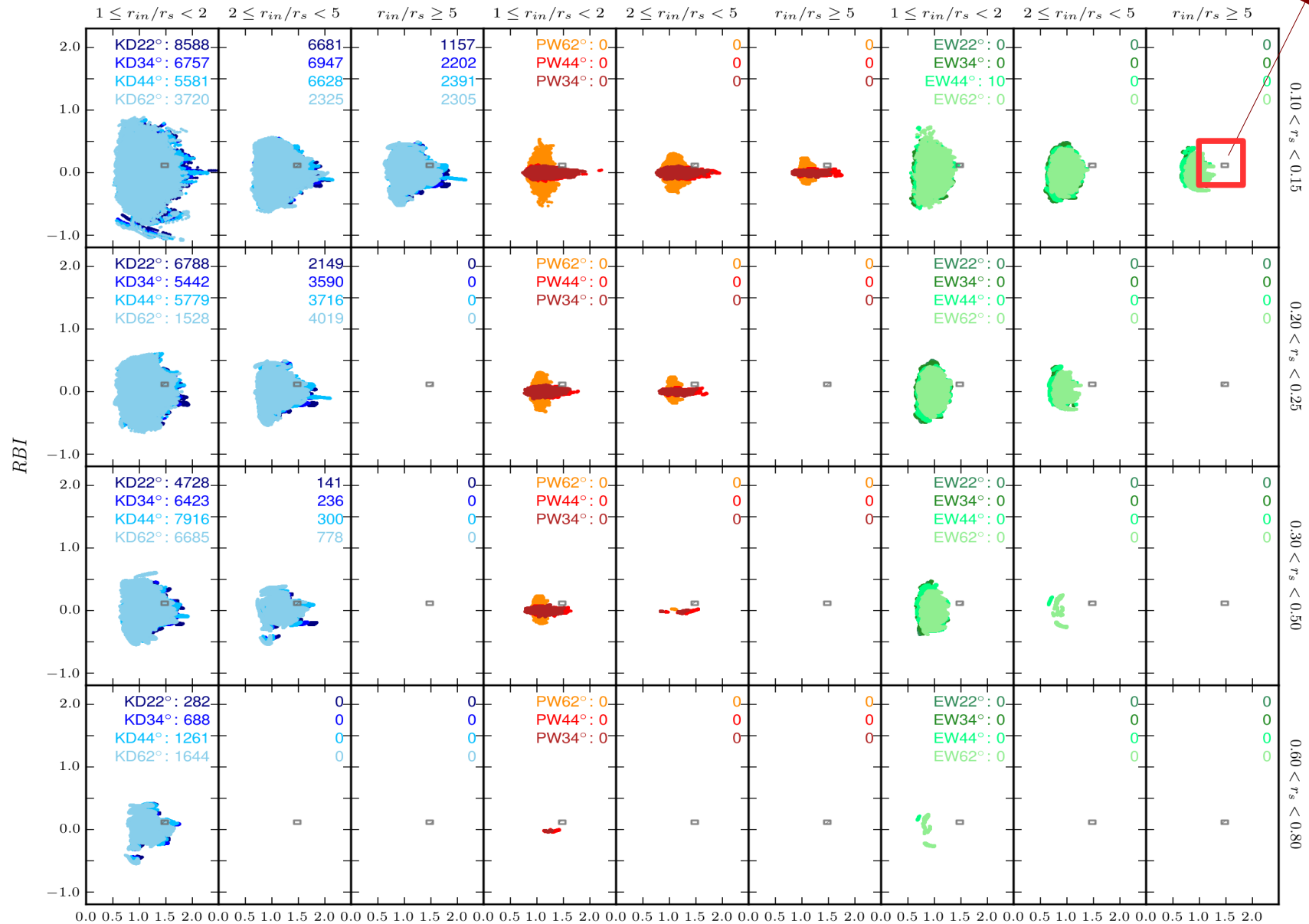
WCI

Confrontation to observations

Modeling the distortions of the H α line profile in O2237+0305A
 Microlensing by a ($\kappa = 0.394, \gamma = 0.395$) caustic network

$2.20 < \mu^{cont} < 2.70, 2.09 < \mu^{BLR} < 2.35$

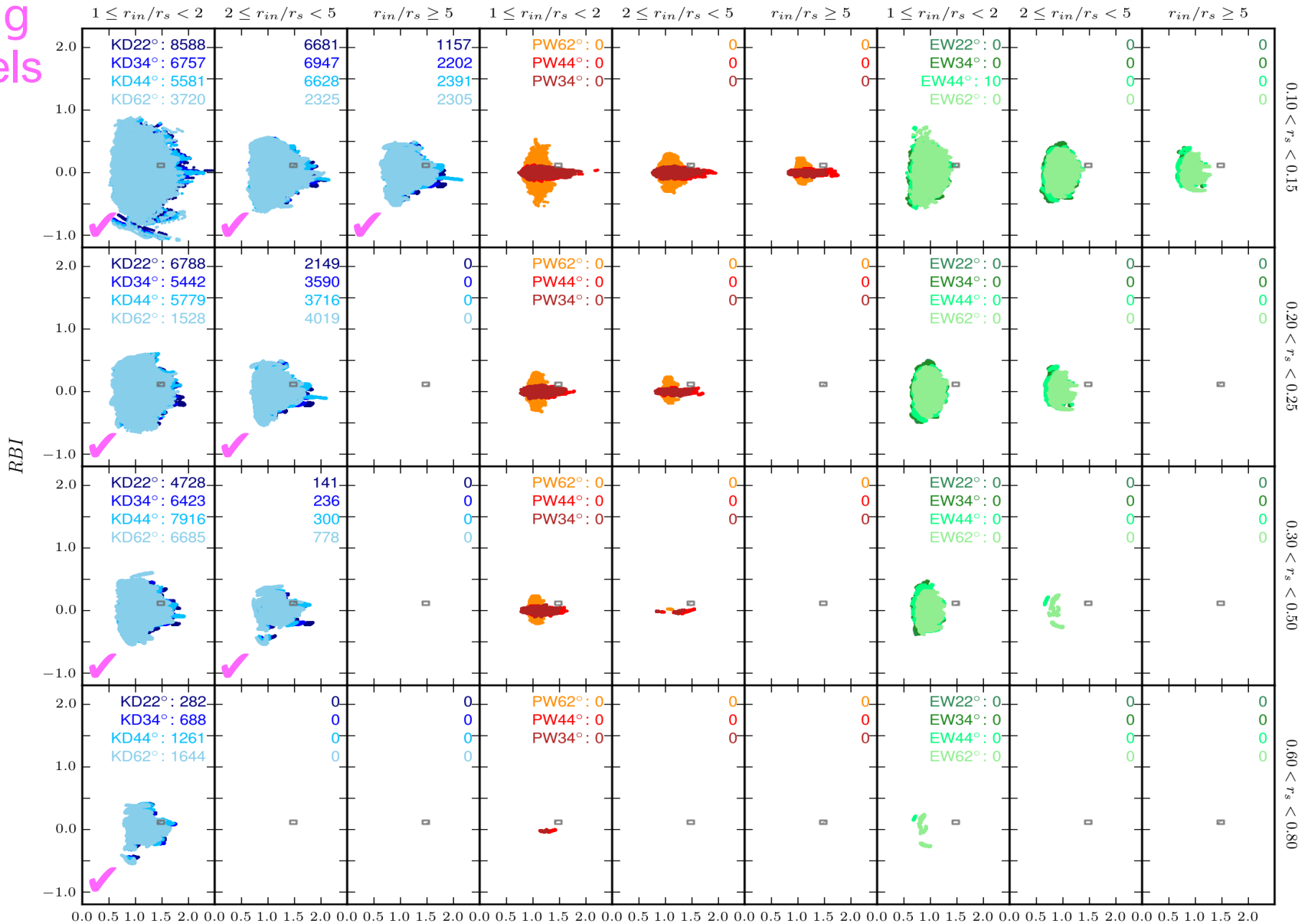
Measured



Confrontation to observations

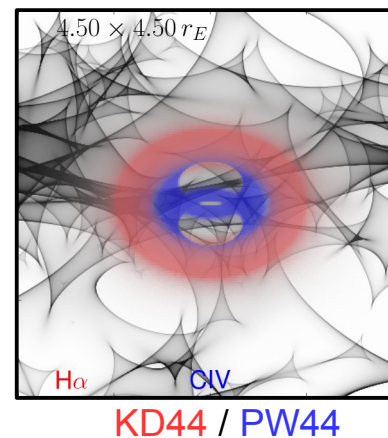
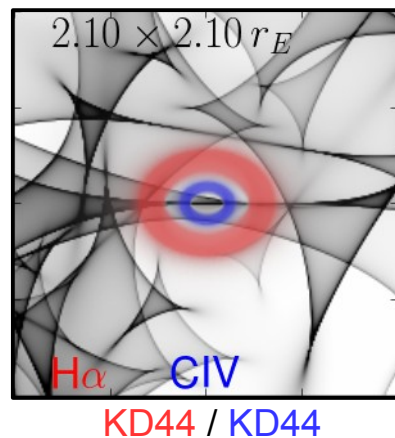
✓
fitting
models

Modeling the distortions of the $H\alpha$ line profile in Q2237+0305A
 Microlensing by a ($\kappa = 0.394, \gamma = 0.395$) caustic network $\rightarrow 2.20 < \mu^{cont} < 2.70, 2.09 < \mu^{BLR} < 2.35$



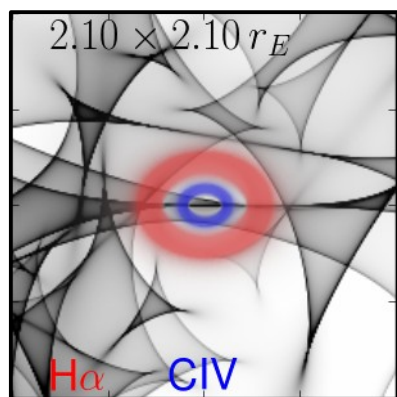
Constraints on the BELR

- *The H α low-ionization region is best represented by a Keplerian Disk in both HE0435-1223 and Q2237+0305*
- *In Q2237+0305, the CIV high-ionization region can be represented by either a Keplerian Disk or a Polar Wind*
- *The H α BELR is larger (x 2) than the CIV BELR*
- *The mean radius of the CIV BELR is 15-50 light-days*
- *Steep emissivity is favored ($\epsilon \sim r^{-3}$)*

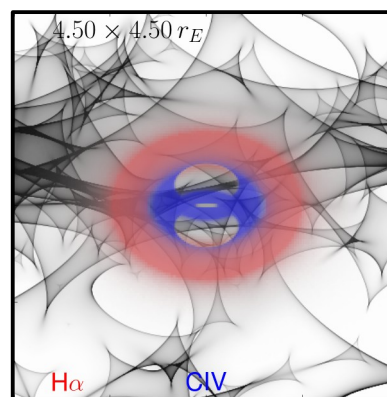


Constraints on the BELR

- *The H α low-ionization region is best represented by a Keplerian Disk in both HE0435-1223 and Q2237+0305*
- *In Q2237+0305, the CIV high-ionization region can be represented by either a Keplerian Disk or a Polar Wind*
- *The H α BELR is larger (x 2) than the CIV BELR*
- *The mean radius of the CIV BELR is 15-50 light-days*
- *Steep emissivity is favored ($\epsilon \sim r^{-3}$)*



KD44 / KD44

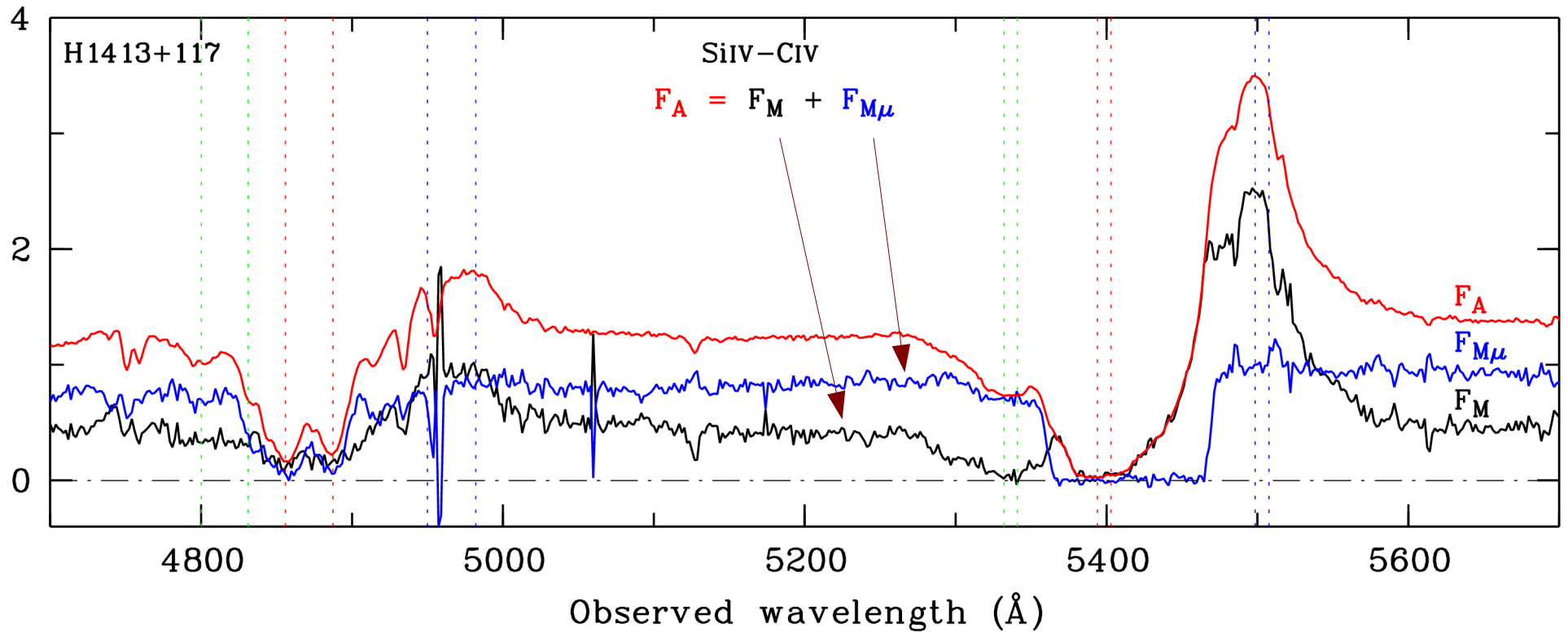


KD44 / PW44

→ *Good constraints on the BELR require a strong microlensing effect and more than a single line observed at a single epoch*

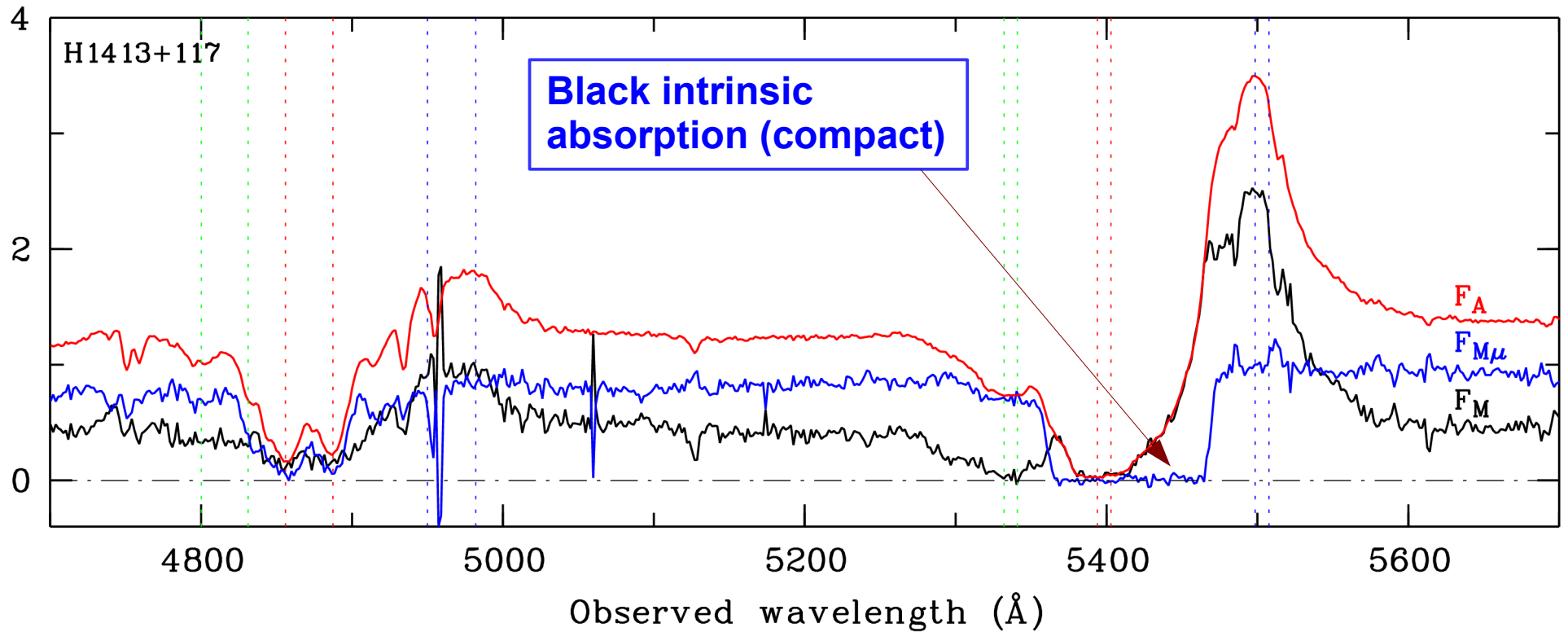
Microlensing in the BAL QSO H1413+117

Strong microlensing in image D and not in image A => disentangling
of the microlensed ($F_{M\mu}$) and non-microlensed spectra (F_M)



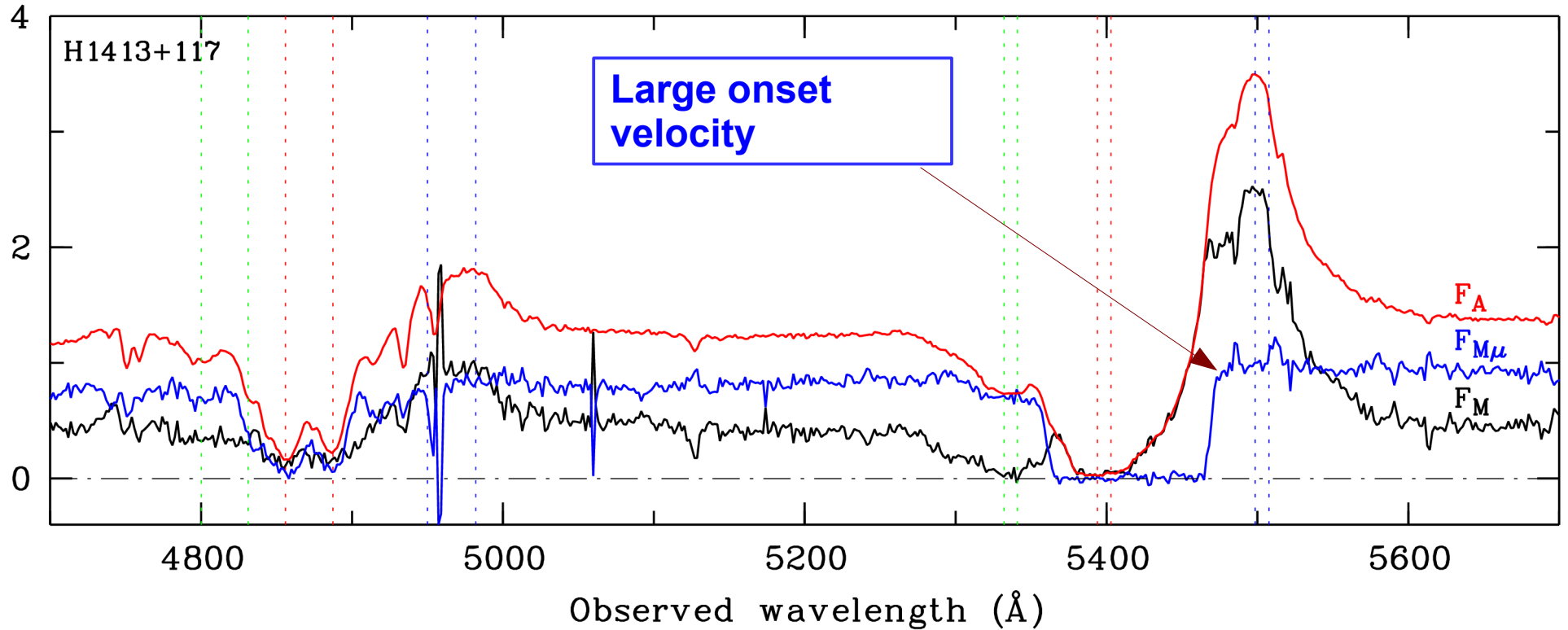
Microlensing in the BAL QSO H1413+117

Strong microlensing in image D and not in image A => disentangling
of the microlensed ($F_{M\mu}$) and non-microlensed spectra (F_M)



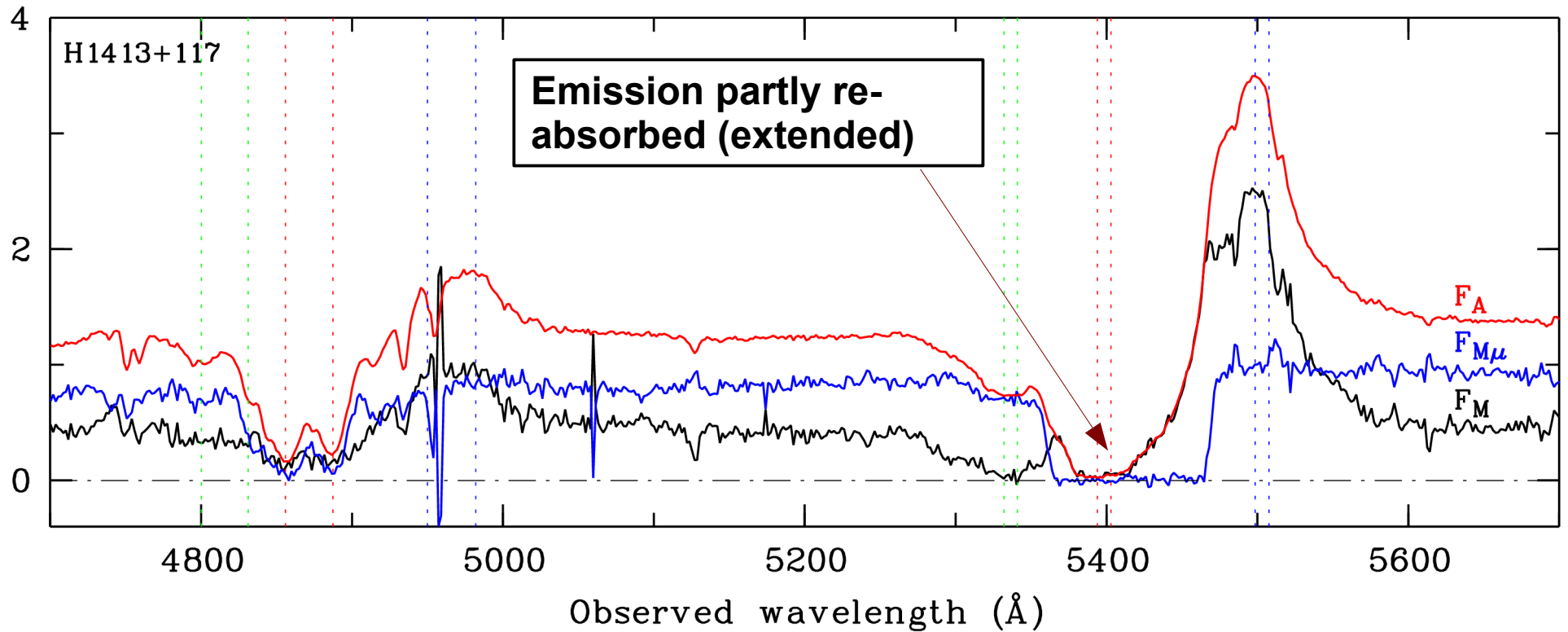
Microlensing in the BAL QSO H1413+117

Strong microlensing in image D and not in image A => disentangling
of the microlensed ($F_{M\mu}$) and non-microlensed spectra (F_M)



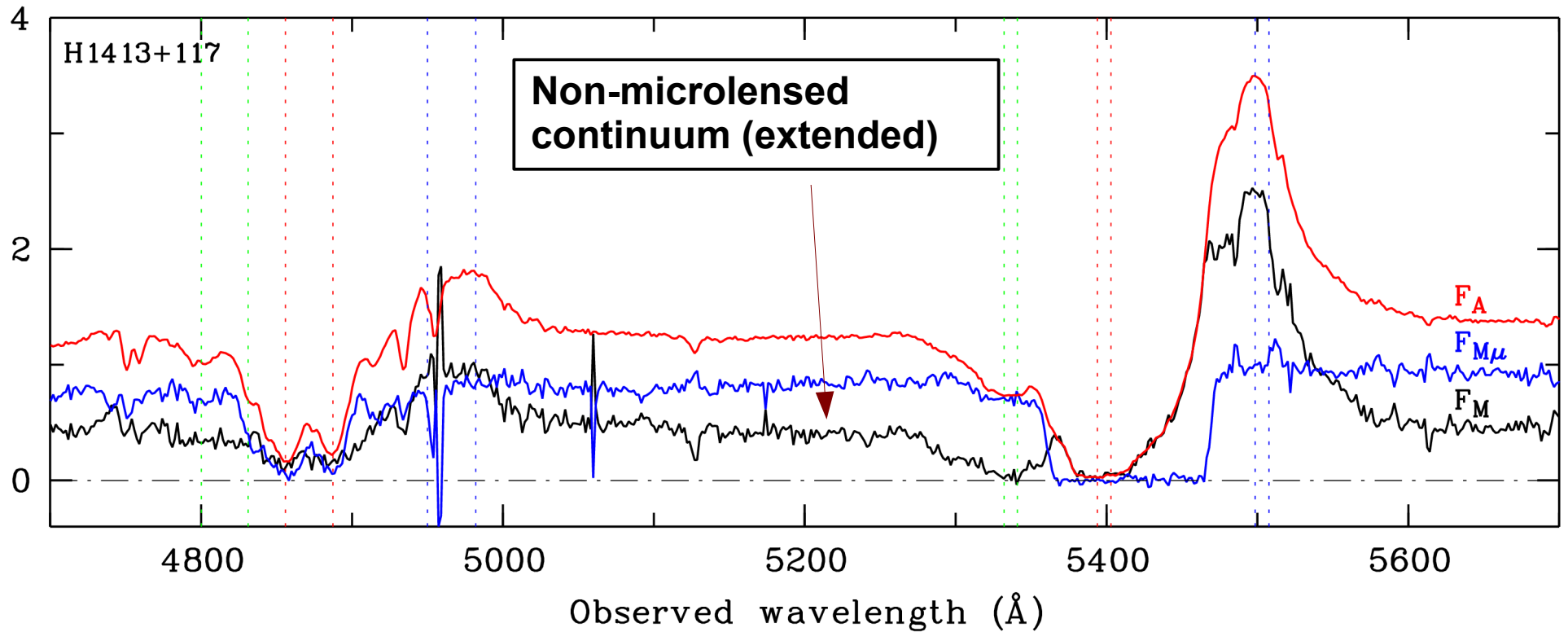
Microlensing in the BAL QSO H1413+117

Strong microlensing in image D and not in image A => disentangling
of the microlensed ($F_{M\mu}$) and non-microlensed spectra (F_M)



Microlensing in the BAL QSO H1413+117

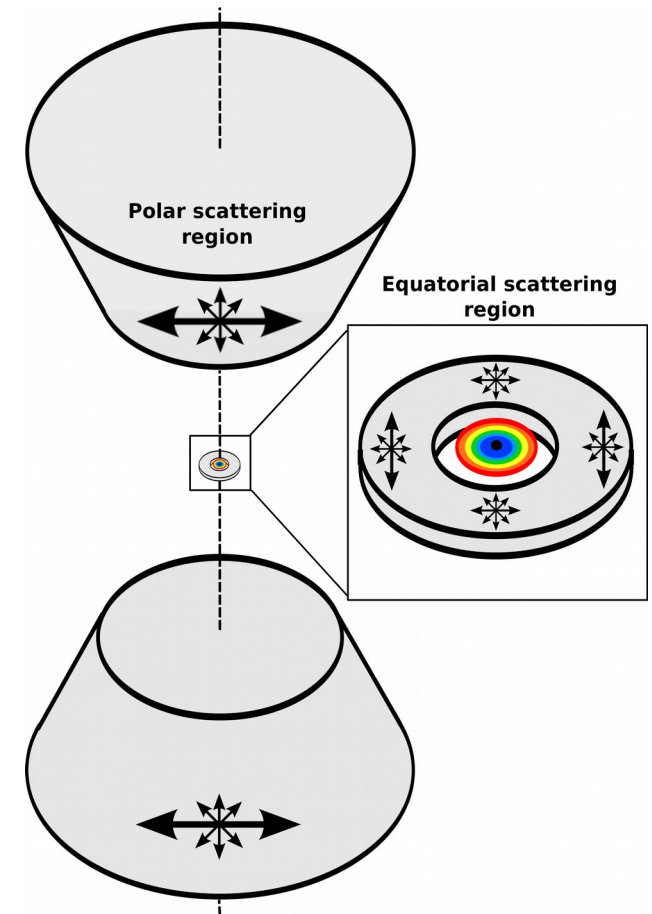
Strong microlensing in image D and not in image A => disentangling
of the microlensed ($F_{M\mu}$) and non-microlensed spectra (F_M)



Microlensing in the BAL QSO H1413+117

- *Evidence for a two-component BAL outflow (polar + disk ?)*
- *Evidence for an extended source of continuum*

→ Microlensing also affect the quasar polarization.
Spectropolarimetry of images D and A suggests that a significant *part of the continuum is polar scattered and “extended”*



Conclusions

- *Microlensing definitely allows to put useful constraints on the BEL and BAL regions in redshift $z \sim 2$ quasars*
- *Comparison with simulations is efficient but shows that strong effects are needed as well as additional constraints (e.g., several lines observed simultaneously, multi-epoch data, independent determination of some parameters, etc).*
- *Up to now, very few objects have been investigated in detail (strong microlensing effects remain rare and unpredictable events)*



Thank you